

Characterization of an original model of myocardial infarction provoked by coronary artery thrombosis induced by ferric chloride in pig

Jean-Michel Dogné^{a,d,1}, Stéphanie Rolin^{b,1}, Michel Péteïn^c, Vincent Tchana-Sato^d, Alexandre Ghuysen^d, Bernard Lambermont^d, Julien Hanson^a, David Magis^d, Patrick Segers^c, Bernard Pirotte^a, Bernard Masereel^b, Pierre Drion^a, Vincent D'Orio^d, Philippe Kolh^d

^aNatural and Synthetic Drugs Research Center, University of Liège, Liège, Belgium

^bDepartment of Pharmacy, University of Namur, Namur, Belgium

^cInstitute of Pathology and Genetics, Lovreval, Belgium

^dHemodynamic Research Center, University Hospital of Liège, Liège, Belgium

^eHydraulics Laboratory, Institute of Biomedical Technology, Ghent University, Sint-Pietersnieuwstraat 41, Gent, Belgium

Abstract

Background: Great advances have been made in the prevention of thrombotic disorders by developments of new pharmacological and surgical treatments. Animal models of arterial thrombosis have largely contributed to the discovery and to the validation of original treatments. The purpose of the present work was to develop and validate an original model of acute myocardial infarction provoked in pig by thrombosis of the left anterior descending (LAD) coronary artery induced by topical application of ferric chloride solution.

Methods and results: Myocardial infarction, resulting from an occlusive and adherent mixed thrombus formed in the LAD coronary artery, was examined at macroscopic level using dual staining technique (Evans blue dye; triphenyltetrazolium chloride) and at microscopic level using conventional histological analyses and immunohistochemical detection of desmin. Biochemical markers (troponin T and ATP), platelet reactivity and standard hemodynamic parameters (such as stroke volume, ejection fraction, stroke work and cardiac output) have also been evaluated. From these analyses, it was demonstrated that each pig developed a transmural area of irreversible damage mainly located in the anteroseptal region of the left ventricle. The more progressive development of coronary artery occlusion, as compared to an abrupt ligation, was accompanied by a correspondingly progressive impairment in hemodynamics.

Conclusion: We conclude that this original porcine model of myocardial infarction is quite close to clinical pathophysiological conditions, such as thrombus formation occurring after atherosclerotic plaque rupture. This certainly constitutes a further argument in favour of this model to assess pharmaceutical or mechanical support of an acutely ischemic heart.

Keywords: myocardial infarction ; thrombosis ; thrombus ; hemodynamics

Introduction

Coronary artery thrombosis is widely accepted as a major cause of myocardial infarction (MI) [1-3]. Indeed, rupture or injury of an atherosclerotic coronary arterial plaque which occurs spontaneously in patients with an acute coronary syndrome or as the result of a percutaneous coronary intervention, serves as a nidus for platelet aggregation and thrombus formation, which, in turn, may cause MI. Since MI was shown to be caused by an acute intracoronary thrombotic occlusion, the primary goal of therapy is rapid, complete, and sustained restoration of infarct-related artery blood flow. Both pharmacological (antiplatelet, anticoagulant and fibrinolytic) and mechanical (Percutaneous Transluminal Coronary Angioplasty) restoration of antegrade coronary blood flow in patients with acute MI have been demonstrated to improve left ventricular function, to reduce infarct size, and to reduce mortality.

The choice of the animal model of thrombosis-induced MI to evaluate the efficiency of antiplatelet, antithrombotic or thrombolytic drugs in pre-clinical studies is crucial. Moreover, the use of experimental models of arterial thrombosis in animals is an obligatory step for the understanding of mechanisms involved in pathologies consecutive to thrombotic disorders. Numerous animal models of thrombosis-induced MI have been proposed in the last decades [4]. Among factors of importance, there are animal species, coronary thrombosis induction method, thrombus composition and site of formation.

In this study, we have developed and validated an original porcine model of acute myocardial infarction provoked by thrombosis of the left anterior descending coronary artery induced by topical ferric chloride

¹ The first two authors have participated equally to this work.

application. Parameters have been evaluated to validate the model, among which the influence of the concentration of ferric chloride solution application, the coronary and myocardial lesions by histopathological and biochemical studies, the platelet reactivity by *ex vivo* platelet aggregation evaluation, and standard hemodynamic parameters.

Materials and methods

Animals and surgical preparation

All experimental procedures and protocols used in this investigation were reviewed and approved by the Ethics Committee of the Medical Faculty of the University of Liège. All procedures conformed to the Guiding Principles in the Care and Use of Animals of the American Physiological Society and were performed according to the Guide for the Care and Use of Laboratory Animals, [NIH publication no. 85-23, revised 1996]. Experiments of thrombus induction were adapted to the pig left anterior descending (LAD) coronary artery from a method of ferric chloride-induced arterial thrombosis first described in rats by Kurz et al., and later applied by Tanaka et al. and Dogné et al. [5-7].

Experiments were performed on 10 healthy pure pietran pigs of either sex weighing from 20 to 30 kg. The animals were premedicated with intramuscular administration of ketamine (20 mg kg⁻¹) and diazepam (1 mg kg⁻¹). Anesthesia was then induced and maintained by a continuous infusion of sufentanil (0.5 µg kg⁻¹ h⁻¹) and pentobarbital (3 mg kg⁻¹ h⁻¹). Spontaneous movements were prevented by pancuronium bromide (0.2 mg kg⁻¹). After endotracheal intubation through a cervical tracheostomy, the pigs were connected to a volume-cycled ventilator (Evita 2, Dräger, Lübeck, Germany) set to deliver a tidal volume of 15 ml kg⁻¹ with a FiO₂ of 0.4 and at a respiratory rate of 20 breaths min⁻¹. End-tidal CO₂ (ET CO₂) measurements (Capnomac, Datex, Helsinki, Finland) were used to monitor the adequacy of ventilation. Respiratory settings were adjusted to maintain ET CO₂ between 30 and 35 mm Hg. Arterial oxygen saturation was closely monitored and maintained above 95% by adjusting the FiO₂ as necessary. Central temperature was measured with a rectal probe and maintained at 37 °C by means of a heating blanket. A standard lead electrocardiogram was used for the monitoring of heart rate (HR).

The chest was entered through median sternotomy, the pericardium was incised and sutured to the chest wall to form a cradle for the heart, and the root of the aorta was dissected clear of adherent fat and connective tissue. A combined conductance-micromanometer catheter (CD Leycom, Zoetermeer, The Netherlands) was inserted through the right carotid artery and advanced into the left ventricle. A micromanometer-tipped catheter (Sentron pressure measuring catheter, Cordis, Miami, FL, USA) was inserted through the right femoral artery and advanced into ascending aorta. A 14-mm diameter perivascular flow-probe (Transonic Systems Inc., Ithaca, NY, USA) was closely adjusted around the aorta 2 cm downstream to the aortic valve. The micromanometer-tipped catheter was manipulated so that the pressure sensor was positioned just distal to the flow probe. Right atrial pressure was measured with a micromanometer-tipped catheter inserted into the cavity through the superior vena cava. A 6F Fogarty balloon catheter (Baxter Healthcare Corp., Oakland, CA, USA) was advanced into the inferior vena cava through a right femoral venotomy. Inflation of this balloon produced a titrable leftward shift in pressure-volume loops by reducing venous return. The jugular vein and the left femoral artery were cannulated for eventual drug administration and for blood samples analysis, respectively.

A segment of the LAD coronary artery was isolated distal to the first diagonal branch for later topical ferric chloride application. An electromagnetic flow probe (Transonic Systems Inc., Ithaca, NY; USA) was placed around the LAD coronary artery 3 cm distal to the site of FeCl₃ application, to measure coronary artery blood flow.

Ferric chloride-induced pig LAD coronary artery thrombosis

After a 30-min stabilisation period, a blood sample was drawn (time 0) and a tissue strip (3 mm width) saturated with ferric chloride solution (20% or 50% w/v) was rolled around the surface of the LAD coronary artery for 45 min and then removed. Animals were kept alive during 6 h following removal of the tissue strip saturated with ferric chloride solution. The blood flow in the LAD coronary artery was monitored throughout the experiment to evaluate the time to occlusion and eventual reperfusion events. At the end of the experiment, area at risk of the left ventricle was determined, ferric chloride-induced thrombosis of the LAD coronary was examined, and myocardial infarction quantified.

Ex vivo platelet aggregation study and platelet count

Ex vivo platelet aggregation and platelet count were measured just before ferric chloride application (time 0) and three times (every 2 h) after tissue strip removal. Blood sample (2.5 ml) was drawn from the catheter inserted in the left femoral artery into a tube containing 0.3 ml of trisodium citrate (3.2% w/v) as an anticoagulant. Platelet-rich plasma (PRP) was prepared by centrifugation at 180 xg for 10 min (15 °C). Platelet-poor plasma (PPP) was

obtained by centrifugation of remaining blood at 2205 g for 10 min (15 °C). The platelet concentration of PRP was measured and adjusted to 3.10^8 cells ml^{-1} by dilution with PPP. Aggregation tests were performed according to Born's turbidimetric method [8] by means of two-channel aggregometer (Chrono-log, Kordia, Leiden, The Netherlands). PPP was used to adjust the photometric measurement to the minimum optical density. PRP (225 μL) was added in a silanised cuvette and stirred (1100 rpm). Platelet aggregation was initiated by addition of arachidonic acid (600 μM final) and ADP (5 μM final). U-46619 was purchased from Cayman Chemicals Company (Ann Arbor, MI, USA). Arachidonic acid and ADP were supplied by Kordia (Leiden, The Netherlands). To evaluate platelet aggregation, the maximum increase in light transmission was determined from the aggregation curve 6 min after addition of the inducer.

Hemodynamic measures

In order to provide similar states of vascular filling, the animals were continuously infused with Ringer lactate ($5 \text{ ml kg}^{-1} \text{ h}^{-1}$), and, when necessary, with hydroxyethylstarch 6% to increase central venous pressure up to 6-7 mm Hg over 30 min. Baseline hemodynamic recording was obtained thereafter from simultaneous measurements of aortic pressure and flow waves. A first diagram of LV pressure-volume relationship was generated from volume and pressure measurements at baseline and after stepwise decreases in preload by reducing venous return. The occlusion was limited to a few seconds in duration in order to avoid reflex responses. All measurements were taken immediately after the animal was briefly disconnected from the ventilator to sustain end-expiration. After deflation of the inferior vena cava balloon, the animals were allowed to rest for an additional 30 min.

Data collection

The conductance catheter was connected to a Sigma-5 signal-conditioner processor (CD Leycom, Zoetermeer, The Netherlands). The ultrasonic flow probe was connected to a flow-meter (HT 207, Transonic Systems Inc., Ithaca, NY, USA), and each micromanometer-tipped catheter to the appropriate monitor (Sentron pressure monitoring, Cordis, Miami, FL, USA). All analog signals and ventricular pressure-volume loops were displayed on screen for continuous monitoring. The analog signals were continuously converted to digital form with appropriate software (Codas, DataQ Instruments Inc., Akron, OH, USA) at a sampling frequency of 200 Hz.

Data analysis

Left ventricular volumes were inferred using the dual field conductance catheter technique (5). Calibration of the conductance signal to obtain absolute volume was performed by the hypertonic saline method (5). Therefore, a small volume (1-2 ml) of 10% NaCl solution was injected into the pulmonary artery during continuous data acquisition. LV contractile function was assessed by the end-systolic pressure-volume relation (ESPVR), and the stroke work (SW).

The instantaneous pressure-volume relationship was considered in terms of a time-varying elastance $E(t)$, defined by the following relationship:

$$E(t) = P(t)/[V(t)-V_d]$$

where $P(t)$ and $V(t)$ are respectively the instantaneous ventricular pressure and volume, and V_d a correction term. End-systole (es) was defined as the instant of time in the ejection phase at which $E(t)$ reaches its maximum, E_{max} . It has been demonstrated that $E(t)$ and V_d are insensitive to preload, at least within physiological ranges (6). Preload was acutely reduced by inflating the inferior vena cava balloon catheter.

Stroke work (SW) was the integrated area of each PV loop.

Effective arterial elastance (E_a) was calculated, in the pressure-volume plane, as the ratio between end-systolic pressure and stroke volume.

Area at risk and infarct size quantifications

Risk area and infarct area were delineated by a dual staining technique [9-12]. After 6 h of ischemia and immediately before the end of the experiment, 20 ml of Evans blue dye solution (0.1 g ml^{-1} in 50 mM phosphate buffered saline, pH 7.4) were injected into the jugular vein, to stain the non-ischemic area blue. The pig was then sacrificed with an intravenous injection of pentobarbital (100 mg kg^{-1}). The heart was then rapidly harvested and sectioned in five transverse slices (0.6 cm thick) from apex to base (S1 to S5). The LV risk area, due to its anatomical dependence on the LAD coronary artery for blood flow, was identified by lack of Evans blue in this region.

Gross slices were photographed with a digital camera (Fujifilm FinePix 2400 Zoom). Morphological changes in size, shape and transmural distribution of myocardial infarction were measured using 2,3,5-triphenyltetrazolium chloride (TTC) staining (Sigma-Aldrich Chemical Co., St. Louis, MO). Tissue slices were rinsed with a cold

isotonic saline solution and then incubated at 38 °C for 15-20 min in a phosphate-buffered solution of TTC (1% in 0.1 M, pH 7.4) [13]. This produced a brick red coloration in the presence of dehydrogenase enzymes in intact myocardium whereas infarcted regions remained unstained due to the collapse of enzyme activity. After photography with a digital camera (Fujifilm FinePix 2400 Zoom), slices of myocardium were placed in 10% neutral-buffered formaldehyde to enhance the contrast between stained and unstained regions. After 3 days of fixation in formalin and just before paraffin proceeding, myocardial sections were again photographed with a video camera (3CCD color video, DXC-390P ExwaveHAD). Infarct size was measured from the tracings of these photographed myocardial slices to a clear acetate sheet and the area of each zone was then weighted. The ratio between the two zones (ischemic area and non-ischemic area) was determined for each slice. Infarct size measured from the tracings of myocardial slices was calculated by planimetry as a percentage of LV mass.

Histopathological examination of ferric chloride-induced coronary artery thrombosis

At the end of the experiment and immediately before TTC staining of the myocardium, the LAD coronary artery was isolated and fixed with 10% neutral-buffered formaldehyde. After 3 days, serial sections of the artery were done and embedded in paraffin. The blocks of artery sections were cut at 6 µm and stained with hematoxylin and eosin. The stained sections were examined at magnifications of x25, x100, x200 and x400 to study thrombus formation and vascular wall structure. Photomicrographs were taken using a Zeiss photomicroscope (Axioscope 2 plus-Sony 3CCD camera, 1024-768 pixels definition).

Histopathological examination of myocardium

After 3 days, three or four tissue-blocks were taken from each slice at standardised locations and routinely processed for paraffin histology. The tissue blocks from myocardium were cut at 6 µm and each section was stained with hematoxylin and eosin, Masson's trichrome and luxol fast blue. The stained sections were examined at magnifications of x25, x100, x200 and x400 to study the distribution of infarction. Photomicrographs were taken using a Zeiss photomicroscope (Axioscope 2 plus-Sony 3CCD camera, 1024-768 pixels definition). In addition, all tissue-blocks of slice S3 were processed for immunohistochemical staining of desmin to investigate cardiac muscle's lesions. Monoclonal antibodies to desmin (clone D33, Biomedica) were diluted 1 /20.

Biochemical markers dosages (cardiac myocytes ATP and plasmatic troponine T levels)

The myocardial ATP content was measured by an adaptation of the ATP bioluminescent assay kit (Sigma-Aldrich diagnostic kit). There is a linear relationship between the relative light intensity generated by luciferin-luciferase reaction and the ATP concentration. Samples of cardiac tissue taken from antero-septal and posterior regions of slice S2 were sequentially frozen in liquid nitrogen and then conserved at -80 °C till ATP dosage. Sample was mechanically disrupted, reduced in powder and then suspended in 700 µl of somatic cell ATP releasing reagent. The suspension was then homogenised with a Dounce (10 times), diluted with ultra pure water and 10 µl added to 100 µl of ATP assay mix (luciferase, luciferin, MgSO₄, EDTA, DTT and BSA in a Tricine buffer). For each sample, luminescence in RLU (Relative Light Unit) was determined with a luminometer (LUMAC Biocounter M2010). Bradford's protein dosage was performed, and results expressed in nmol ATP g⁻¹ of protein. Plasma troponine T (TnT) concentration was measured from arterial blood samples taken at 0, 3 and 6 h after inducing LAD occlusion with ferric chloride. Collected samples were centrifuged at 2205 xg for 10 min at 15 °C. The supernatant was removed and plasma concentration of TnT measured [14]. The area under the curve (AUC) is expressed in µg ml⁻¹ h⁻¹.

Statistics

Results are expressed as the mean ± standard error of the mean (SEM) and statistical significance was determined by Student's t-test and chi-square test. Probability values of less than 0.05 were considered to be significant.

Furthermore, time evolution of hemodynamic parameters was investigated by means of a longitudinal mixed effects model. Basic fitted models are of the form

$$Y_{ij} = \alpha + \beta t_i + -\gamma t_i^2 + b_{j0} + b_{j1} t_i + b_{j2} t_i^2 + \epsilon_{ij}$$

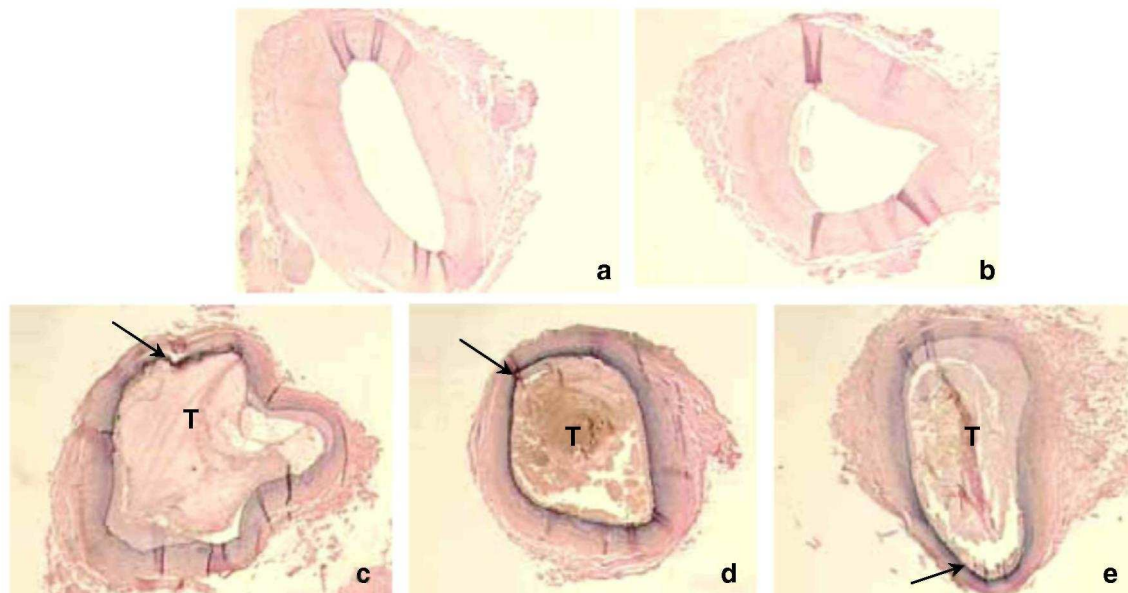
where Y_{ij} is response parameter measured at time t_i on subject (pig) j , α , β and γ are fixed effects for the mean parameter evolution; b_{j0} , b_{j1} and b_{j2} are subject-specific random effects; and ϵ_{ij} is the measurement error. Estimation about both fixed and random effects were performed using SAS software (SAS Institute Inc., Cary, NC, USA). Approximate F-tests (at 5% significance level) were used to assess potential mean evolution of the response with time. Therefore, p -value <0.05 refers to significant non-constant time trend of parameter values.

Results

Effect of the concentration of ferric chloride solution application on the LAD coronary artery blood flow

Two concentrations of ferric chloride solutions have been used to saturate the tissue strip (3 mm width) that was rolled around the surface of the LAD coronary artery: 20% and 50% (w/v). The blood flow in the LAD coronary artery was monitored throughout the experiment. The 20% ferric chloride solution failed to lead to an occlusion of the LAD coronary artery in all animals within 45 min. In contrast, the 50% ferric chloride solution induced a complete occlusion of the LAD coronary artery in all animals within that same period of time (Fig. 1). The mean LAD coronary artery blood flow measured at baseline was $42.3 \pm 1.6 \text{ ml min}^{-1}$ and the average occlusion time $23.2 \pm 1.2 \text{ min}$. In 6 of 10 pigs, the LAD coronary artery blood flow linearly decreased to zero, while in the four other animals reperfusion episodes occurred before reaching a complete occlusion within 30 min. The tissue strip saturated with the 50% ferric chloride solution was removed from the artery after 45 min and no reperfusion events occurred within the next 6 h.

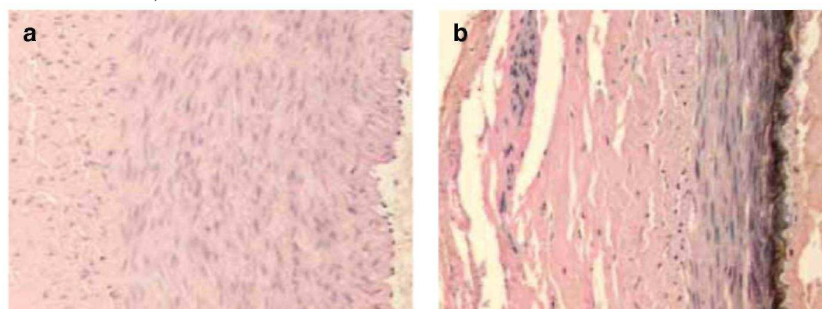
Figure 1 - Light micrographs of serial sections of LAD coronary artery showing ferric chloride-induced thrombi (T) in pictures (c), (d) and (e). Thrombus is indicated on picture by letter T and arrows indicate ferric chloride contact. Sections represented in pictures (a) and (b) showing intact coronary artery were taken just above application of ferric chloride. All sections were stained with hematoxylin and eosin (x25).



Histopathological examination of ferric chloride-injured LAD coronary artery

Topical application of tissue strip saturated with 50% ferric chloride solution to the LAD coronary artery provoked vascular injury responsible for occlusive mixed thrombi. All three layers which constitute a healthy vessel wall (intima, media and adventice) were damaged at the site of tissue strip application (Fig. 2). The mixed thrombi, composed of both fibrin and platelets, were adherent to the vessel wall at the site of ferric chloride contact as revealed by light micrographs of all artery sections stained with hematoxylin-eosin.

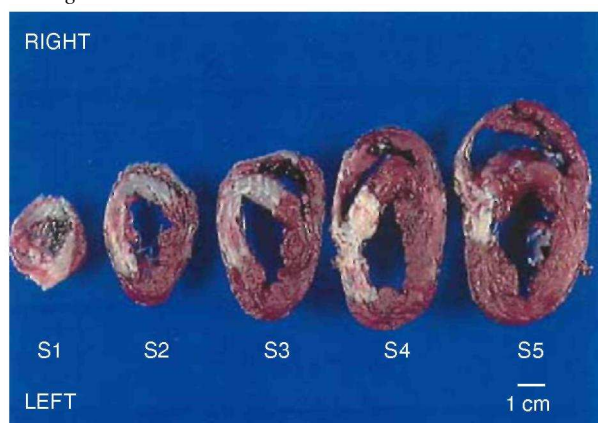
Figure 2 Structure of normal vessel wall (a) compared to injured vessel wall due to ferric chloride contact (b) (Hematoxylin and eosin, x200).



Macroscopy and infarct size

All animals enrolled in this study of coronary artery thrombosis induced by topical ferric chloride application developed a transmural area of irreversible damage, mainly located in the antero-septal region of the left ventricle, within 6-h following tissue strip removal. The infarct zone was delineated for each heart by TTC staining which revealed a collapse of the dehydrogenase system (Fig. 3). The calculated infarct size was expressed as the percentage of LV mass and was calculated by planimetry from heart slices (S1 to S5). The mean infarct size was $35.3 \pm 2.1\%$ reported to the LV mass. The risk area revealed by Evans blue dye was $36.9 \pm 2.1\%$ of the LV mass. For each pig, risk area revealed by Evans blue was superimposed to the necrotic zone revealed by TTC staining.

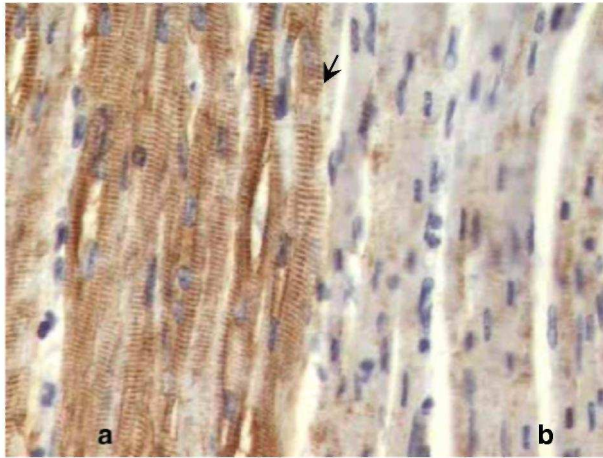
Figure 3 - Photograph of gross slices (S1—S5) of porcine heart after TTC staining from animals with an occlusive thrombus in the LAD coronary artery induced by ferric chloride. Distinct delineation of antero-septal infarction is visible by lack of staining.



Histopathological examination of infarcted myocardium

Hearts were examined by light microscopy. The main ischemic changes were observed in the LV anterior wall, corresponding to the area supplied by the LAD coronary artery. Pyknosis of nuclei from muscle fibres, oedema and beginning leucodiapedesis from the capillaries suggested that these cells reached the stage of necrosis. If histological diagnosis could be established with hematoxylin and eosin staining, delineation between ischemic and non-ischemic region was unclear. For this reason, desmin immunohistochemical staining was used to microscopically detect the necrotic zone [15]. Loss of staining with antibodies to desmin was detected in necrotic myocardium and closely related to the affected area revealed by TTC staining. In healthy myocardial regions, positive immunohistological staining of desmin revealed the Z bands of cardiac muscle cells giving a typical striated appearance (Fig. 4). The pattern and distribution of infarction identified histologically was related to the results obtained by TTC staining.

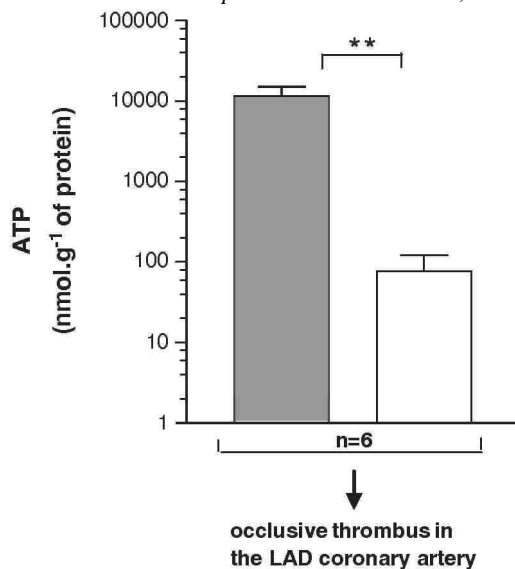
Figure 4 Distinct delineation (arrow) between healthy myocardial muscle with typical striated appearance (a) and necrotic myocardial muscle (b) from heart suffering of 6 h ischemia after immunohistochemical detection of desmin. Positive detection of desmin corresponds to healthy region (brown) (a) while negative detection corresponds to necrotic region (x400). (For interpretation of the references to colour in this figure legend, the reader is referred to the web version of this article.)



Cardiac myocytes ATP and plasmatic troponine T levels

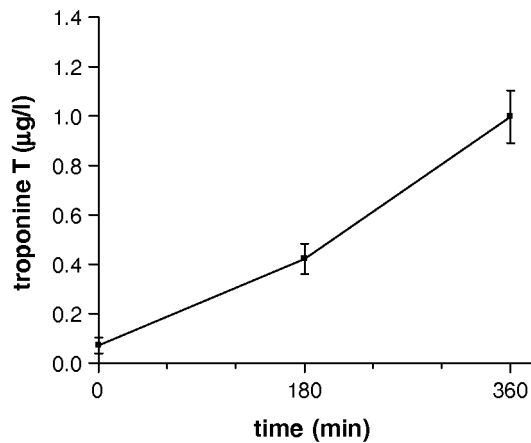
ATP depletion is one of the main biochemical consequence of myocardial ischemia [16]. For this reason, ATP concentration was measured in myocardium from all animals. Two samples were judiciously taken from slice n°2 (S2) of each heart: one in the anteroseptal region and one in the posterior region stained by TTC (Fig. 5). In all animals, a significant ($P < 0.01$) myocardial ATP decrease was observed in the necrotic region (76.6 ± 43.6 nmol g^{-1} vs 11630 ± 3410 nmol g^{-1} of protein).

Figure 5 - ATP contents (nanomoles g^{-1} of protein) of anteroseptal and posterior samples from heart slice n° 2 (S2) from 6 animals. Results are expressed as mean \pm S.E.M.; $**P < 0.01$.



Plasmatic levels of troponine T were measured as a specific biochemical marker of acute myo-cardial infarction [17]. In healthy pigs, TnT averaged concentration was inferior to $0.1 \mu g l^{-1}$. In our experiments, TnT level was $0.071 \pm 0.031 \mu g l^{-1}$ at time 0. A significant elevation of TnT concentration was observed after topical application of ferric chloride to the coronary artery and throughout the 6 h of ischemia to reach $0.997 \pm 0.106 \mu g l^{-1}$ (Fig. 6).

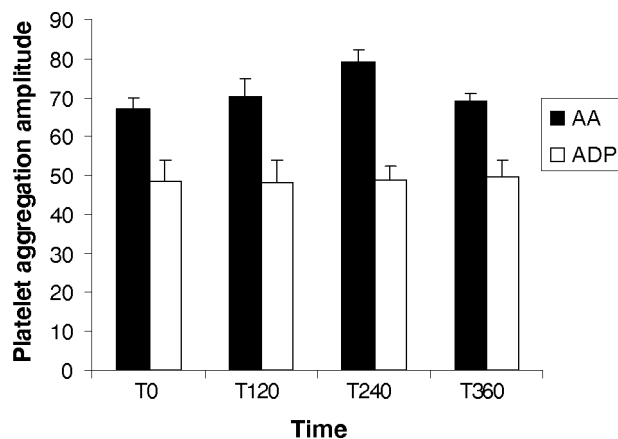
Figure 6 - Troponine T concentration ($\mu\text{g l}^{-1}$) throughout the experiment. Measures were done at 0, 180 and 360 min after topical application of ferric chloride to the LAD coronary artery. Results are expressed as mean \pm S.E.M.



Ex vivo platelet aggregation study and platelet count

Blood samples were collected and platelet-rich plasma prepared. A mild drop in platelet count of PRP was observed in all animals throughout the experiment. Using light transmission aggregometry, the extent of aggregation induced by platelet agonists (arachidonic acid and ADP) was determined on PRP adjusted to $3 \cdot 10^8$ cells. ml^{-1} by dilution with PPP. Ex vivo platelet aggregation measured just before ferric chloride application (time 0) and three times (every 2 h) after tissue strip removal remained maximum with the two inducers used (Fig. 7).

Figure 7 - Ex vivo platelet aggregation induced by arachidonic (600 μM) and ADP (5 μM) measured just before ferric chloride application (T0) and three times (every 2 h: T120, T240 and T360) after removal of tissue strip soaked with 50% (w/v) ferric chloride solution.



Hemodynamic measures

LAD coronary artery occlusion induced a significant decrease in aortic blood flow, from 57.8 ± 5.9 ml s^{-1} at baseline to 47.3 ± 4.9 ml s^{-1} at T180 ($p < 0.05$), while aortic pressure remained statistically unchanged (Fig. 8). As illustrated in Fig. 9, the decrease in cardiac output was due to a major drop in stroke volume SV (from 36.9 ± 2.1 ml at baseline to 22.9 ± 2.9 ml at T180, $p < 0.001$), while heart rate significantly increased (from 107 ± 6 beats min^{-1} at baseline to 142 ± 11 beats min^{-1} at T180, $p < 0.001$).

The impairment in left ventricular function was expressed by a significant decrease in both ejection fraction EF (from $61 \pm 8\%$ at baseline to $49 \pm 4\%$ at T180, $p < 0.001$), and stroke work (from 3069 ± 141 mm Hg ml at baseline to 1774 ± 268 mm Hg ml at T180, $p < 0.001$), at unchanged end-diastolic volume. However, end-systolic elastance E_{es} remained statistically unchanged, while effective arterial elastance E_{a} raised throughout the experiment, from 2.6 ± 0.4 mm Hg ml^{-1} at baseline to 4.3 ± 0.7 mm Hg ml^{-1} at T180 ($p < 0.01$) (Fig. 9).

Figure 8 - Evolution of mean aortic pressure (P_{mean}), mean aortic flow (Q_{mean}), heart rate (HR), and effective arterial elastance (E_a) throughout the experiment. The tissue strip saturated with $FeCl_3$ was placed around the LAD coronary artery immediately after baseline measurements (T0) and removed after 45 min.

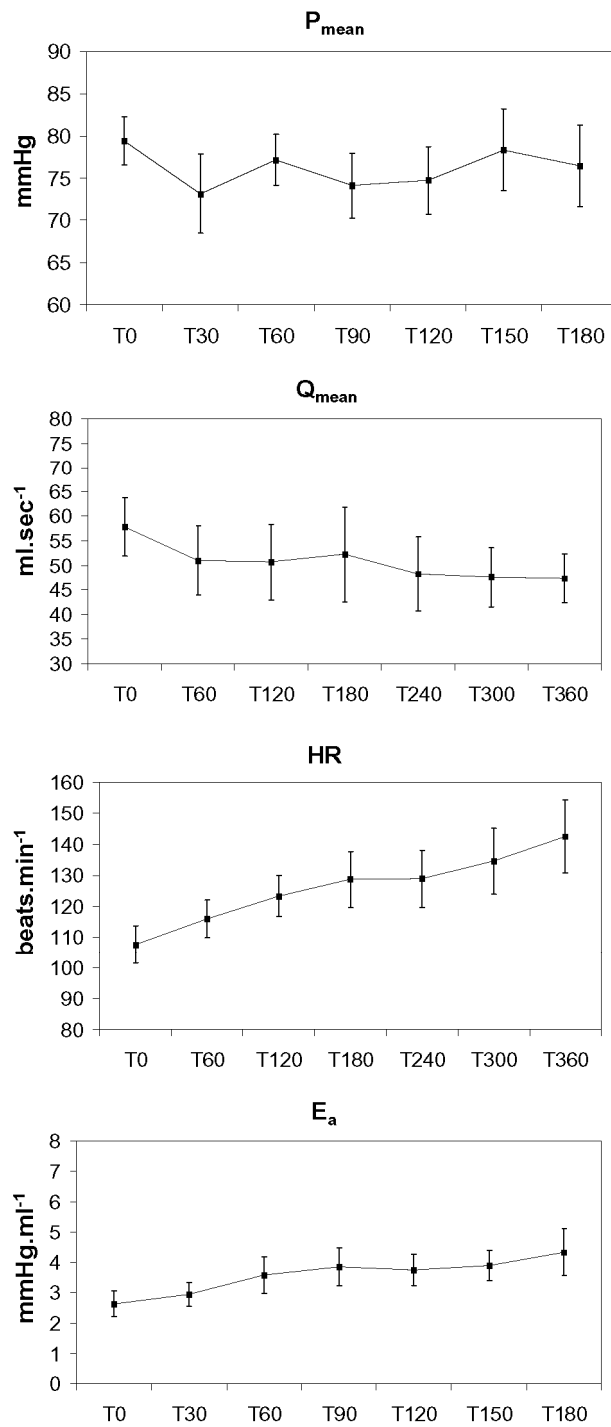
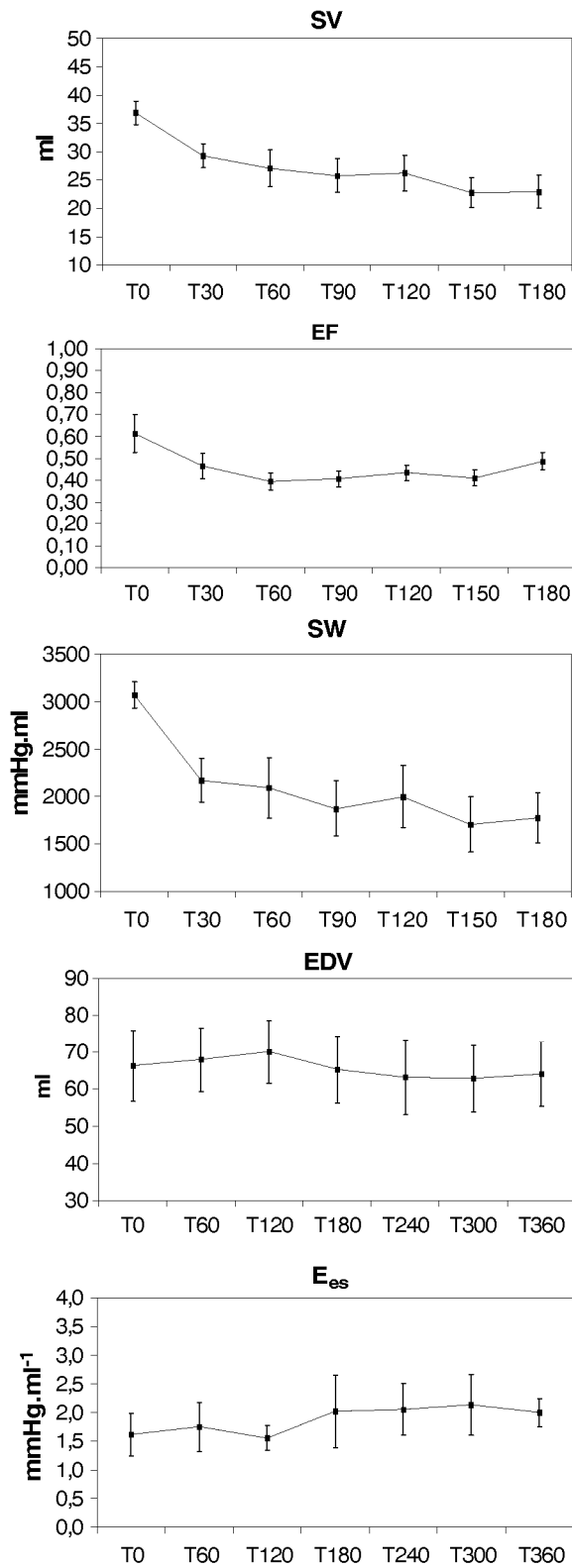


Figure 9 - Evolution of stroke volume (SV), ejection fraction (EF), stroke work (SW), end-diastolic volume (EDV), and end-systolic elastance (E_{es}) throughout the experiment. The tissue strip saturated with $FeCl_3$ was placed around the LAD coronary artery immediately after baseline measurements (T0) and removed after 45 min.



Discussion

Many animal models of myocardial infarction induced by coronary artery injury have been reported in the literature but few have been fully validated. In this study, we aimed to describe an original model of thrombosis-

induced MI in the pig. We chose to induce an arterial wall lesion by topical application of ferric chloride solution. Indeed, this technique has already been reported to induce arterial thrombosis in the rat and appeared of great interest. Thus, Kurtz et al. first produced a small animal model of arterial thrombosis for study of novel antithrombotic agents [5]. The rat carotid artery was injured by topical application of a ferric chloride solution. The results demonstrated that FeCl_3 dose-dependently provoked endothelial damage and induced formation of an occlusive thrombus composed of activated platelets, fibrin strands and entrapped erythrocytes [5]. This original technique was also applied recently by other researchers to induce arterial or venous thrombosis in small animals such as the mouse [18-19]. This offers the possibility to work on genetically modified animals [20-23]. Moreover, the small size of mice also offers an advantage to investigators studying the *in vivo* effects of compounds that are expensive or difficult to produce in large quantities. However, the small size of mice also poses considerable technical difficulties to those attempting to model human vascular disorders.

To our knowledge, the use of ferric chloride to induce coronary thrombosis in the dog or pig has never been reported and validated. Frequently used arterial wall lesion models to induce coronary thrombosis in these species are parietal injury with a needle associated with arterial stenosis (Folts' model) [24-26] and electrolytic injury [27,28]. All these models are considered as representative of the thrombotic reaction occurring after atherosclerotic plaque rupture leading in most cases to myocardial infarction [29].

In this study, we demonstrated that the original porcine model of myocardial infarction where thrombus formation is induced by ferric chloride topical application to the LAD coronary artery, is a suitable model. First, we tested two concentrations of ferric chloride solution used to soak the tissue strip (3 mm width) that was rolled around the surface of the LAD coronary artery. Indeed, in previous studies performed on the rat abdominal aorta and on the mouse carotid artery, several concentrations of ferric chloride solution (10-50%) were described to trigger thrombus formation. While, in our study, the 20% ferric chloride solution did not lead to an occlusion of the LAD coronary artery, the 50% ferric chloride solution induced a complete occlusion within 45 min. Thus, as already observed on arteries of small animals, we confirmed that the rate of thrombus formation depends on the concentration of ferric chloride. Embolization of transiently occlusive thrombi can occur, producing cyclic flow variation in the LAD coronary artery. However, in this model, the time to occlusion with a 50% solution was reproducible (23.2 ± 1.2 min). This "outside-inside" form of injury produced transmural cell necrosis and disrupted the integrity of the vascular endothelium. Indeed, histopathological examination of the LAD coronary artery showed that ferric chloride was responsible for disturbing vessel wall integrity leading to an occlusive mixed thrombus enriched in platelets and fibrin. The precise mechanism by which ferric chloride triggers thrombosis is not well defined, since simple endothelial denudation does not necessarily trigger occlusive thrombosis [30].

Occlusive thrombi formed due to ferric chloride contact and observed in all coronary artery photomicrographs, were responsible for the installation of a major myocardial infarction located in the anteroseptal region of myocardium. To be quantified, MI was examined on macroscopical, microscopical and biochemical levels.

Thus, MI was macroscopically delineated by TTC staining which coloured in brick red healthy regions due to the reaction with intact dehydrogenase enzymes while infarcted region appeared uncoloured. In all animals, occlusion of the LAD coronary artery provoked by ferric chloride at the same anatomical site induced an infarct of $35.1 \pm 2.1\%$ of LV mass. Area at risk evidenced by Evans blue dye was similar and could be superposed to the infarct zone revealed by TTC staining. These results can be explained by the pig coronary collateral system less developed than in humans, in whom necrosis progression occurs only after 6-12 h. Histopathological examination of myocardium suffering 6 h of ischemia showed evidence of the effect of anoxia with several alterations consisting of interstitial oedema, granularity, small leukocytes infiltrates, anisonucleosis, and caryolysis. Myocardial infarction was clearly delineated by the lack of TTC staining and there was a close correspondence between gross and histological measurements of necrosis area in each slice. Moreover, clear delineation between healthy and ischemic myocardium revealed on gross slices was clearly seen in desmin stained sections and could be superimposed.

Several biochemical markers were also studied. Drop of myocardial ATP content is an indicator of tissue necrosis [12,31]. In the anteroseptal region, a significant ATP depletion was measured. Plasma dosage of TnT, a sensitive and specific biological marker of necrosis, revealed a marked and significant rising of this marker throughout 6 h of ischemia.

We also evaluated the impact of the thrombus formation in the LAD coronary artery by ferric chloride application on circulating platelets and hemodynamic parameters. Thus aggregometry studies were performed on PRP obtained from systemic blood. Two inducers were used, arachidonic acid which triggers platelet aggregation by the release of thromboxane A_2 and ADP which activates platelets after binding to a purinergic receptor present at their surface. *Ex vivo* platelet aggregation measured just before ferric chloride application (time 0) and three times (every 2 h) after tissue strip removal remained maximum with the two inducers used.

This result and the observation that only a mild drop in the blood platelet count was observed throughout the experiment indicated that the thrombus formation remained located in the LAD coronary artery and that circulating platelets can still be stimulated.

The significant decrease in hemodynamic parameters, such as stroke volume, ejection fraction, stroke work and cardiac output, was in accordance with the development of an acute myocardial infarction. Further, the more progressive development of coronary artery occlusion, as compared to an abrupt ligation, was accompanied by a correspondingly progressive impairment in hemodynamics. This certainly constitutes a further argument in favour of this model, for example to assess pharmaceutical or mechanical support of an acutely ischemic heart.

From these experiments, we conclude that this original porcine model of myocardial infarction induced by topical application of ferric chloride to the LAD coronary artery is quite close to clinical pathophysiological conditions, such as thrombus formation occurring after atherosclerotic plaque rupture. This model has the advantage that no specialized equipment is necessary to induce thrombosis. However, some limitations of this model should be pointed out. First, we are aware of the fact that the maintenance of pigs is expensive and difficult, and requires special facilities that are beyond the capabilities of most laboratories. Secondly, the pig presents a high myocardial sensitivity to hypoxia. Acute reduction of coronary blood flow can easily induce paroxysmic ventricular fibrillation which may then require the use of prophylactic antiarrhythmic agents.

Acknowledgements

The authors thank Mrs Michaela Oana, MD., for advice on this experiment, Mrs Carine Michiels, PhD., for helping in ATP dosage, and Mrs Cécile Meraglia for excellent technical assistance.

References

- [1] DeWood MA, Spores J, Notske R, Mouser LT, Burroughs R, Golden MS, et al. Prevalence of total coronary occlusion during the early hours of transmural myocardial infarction. *N Engl J Med* 1980;303:897-902.
- [2] Davies MJ, Thomas A. Thrombosis and acute coronary artery lesions in sudden cardiac ischemic death. *N Engl J Med* 1984;310:1137-40.
- [3] Tofler GH, Brezinski D, Schafer AL, Czeisler CA, Rutherford JD, Willich SN, et al. Concurrent morning increase in platelet aggregability and the risk of myocardial infarction and sudden cardiac death. *N Engl J Med* 1987;316:1514-8.
- [4] Leadley Jr RJ, Chi L, Rebello SS, Gagnon A. Contribution of in vivo models of thrombosis to the discovery and development of novel antithrombotic agents. *J Pharmacol Toxicol Methods* 2000;43:101-16.
- [5] Kurz KD, Main BW, Sandusky GE. Rat model of arterial thrombosis induced by ferric chloride. *Thromb Res* 1990;60: 269-80.
- [6] Tanaka T, Sato R, Kurimoto T. Z-335, a new thromboxane A₂ receptor antagonist, prevents arterial thrombosis induced by ferric chloride in rats. *Eur J Pharmacol* 2000;401:413-8.
- [7] Dogne JM, Hanson J, de Levai X, Kolh P, Tchana-Sato V, de Levai L, et al. Pharmacological characterization of *N-tert-butyl-N'*-[2-(4'-methylphenylamino)-5-nitrobenzenesulfonyl]urea (BM-573), a novel thromboxane A₂ receptor antagonist and thromboxane synthase inhibitor in a rat model of arterial thrombosis and its effects on bleeding time. *J Pharmacol Exp Ther* 2004;309:498-505.
- [8] Born GV, Cross MJ. The aggregation of blood platelets. *J Physiol* 1963;168:178-95.
- [9] Warltier DC, Zyvoloski MG, Gross GJ, Hardman HF, Brooks HL. Determination of experimental myocardial infarct size. *J Pharmacol Methods* 1981;6:199-210.
- [10] Toki Y, Hieda N, Okumura K, Hashimoto H, Ito T, Ogawa K, et al. Myocardial salvage by a novel thromboxane A₂ synthetase inhibitor in a canine coronary occlusion-reperfusion model. *Arzneimittelforschung* 1988;38:224-7.
- [11] Higo K, Karasawa A, Kubo K. Early thrombolysis by recombinant tissue-plasminogen activator is beneficial to the ischemic myocardium. *J Pharmacobio-dyn* 1992;15: 33-7.
- [12] Rolin S, Petein M, Tchana-Sato V, Dogne JM, Benoit P, Lambermont B, et al. BM-573, a dual thromboxane synthase inhibitor and thromboxane receptor antagonist, prevents pig myocardial infarction induced by coronary thrombosis. *J Pharmacol Exp Ther* 2003;306:59-65.
- [13] Fishbein MC, Y-Rit J, Lando U, Kanmatsuse K, Mercier JC, Ganz W. The relationship of vascular injury and myocardial hemorrhage to necrosis after reperfusion. *Circulation* 1980;62:1274-9.
- [14] Lauer B, Niederau C, Kuhl U, Schannwell M, Pauschinger M, Strauer BE, et al. Cardiac troponin T in patients with clinically suspected myocarditis. *J Am Coll Cardiol* 1997;30:1354-9.
- [15] Vargas SO, Sampson BA, Schoen FJ. Pathologic detection of early myocardial infarction: a critical review of the evolution and usefulness of modern techniques. *Mod Pathol* 1999;12:635-45.
- [16] Opie LH. New concepts regarding events that lead to myocardial infarction. *Cardiovasc Drugs Ther* 1995;9(Suppl 3):479-87.
- [17] Chapelle JP. Cardiac troponin I and troponin T: recent players in the field of myocardial markers. *Clin Chem Lab Med* 1999;37:11-20.
- [18] Chen C, Li Q, Darrow AL, Wang Y, Derian CK, Yang J, et al. Mer receptor tyrosine kinase signaling participates in platelet function.

Arterioscler Thromb Vasc Biol 2004;24: 1118-23.

- [19] Pan S, Kleppe LS, Witt TA, Mueske CS, Simari RD. The effect of vascular smooth muscle cell-targeted expression of tissue factor pathway inhibitor in a murine model of arterial thrombosis. *Thromb Haemost* 2004;92:495-502.
- [20] Pynn M, Schafer K, Konstantinides S, Halle M. Exercise training reduces neointimal growth and stabilizes vascular lesions developing after injury in apolipoprotein e-deficient mice. *Circulation* 2004;109:386-92.
- [21] Schafer K, Konstantinides S, Riedel C, Thinner T, Muller K, Delias C, et al. Different mechanisms of increased luminal stenosis after arterial injury in mice deficient for urokinase- or tissue-type plasminogen activator. *Circulation* 2002;106:1847-52.
- [22] Weiss EJ, Hamilton JR, Lease KE, Coughlin SR. Protection against thrombosis in mice lacking PAR3. *Blood* 2002;100:3240-4.
- [23] Zeng B, Bruce D, Kril J, Ploplis V, Freedman B, Brieger D. Influence of plasminogen deficiency on the contribution of polymorphonuclear leucocytes to fibrin/ogenolysis: studies in plasminogen knock-out mice. *Thromb Haemost* 2002;88:805-10.
- [24] Wu D, Vanhoorelbeke K, Cauwenberghs N, Meiring M, Depraetere H, Kotze HF, et al. Inhibition of the von Willebrand (VWF)—collagen interaction by an antihuman VWF monoclonal antibody results in abolition of in vivo arterial platelet thrombus formation in baboons. *Blood* 2002;99:3623-8.
- [25] Sill JC, Bertha B, Berger I, Uhl C, Nugent M, Folts J. Human platelet Ca²⁺ mobilization, glycoprotein IIb/IIIa activation, and experimental coronary thrombosis in vivo in dogs are all inhibited by the inotropic agent amrinone. *Circulation* 1997;96:1647-53.
- [26] Demrow HS, Slane PR, Folts JD. Administration of wine and grape juice inhibits in vivo platelet activity and thrombosis in stenosed canine coronary arteries. *Circulation* 1995;91: 1182-8.
- [27] Hennen JK, Huang J, Barrett TD, Driscoll EM, Widens DE, Park AM, et al. Effects of selective cyclooxygenase-2 inhibition on vascular responses and thrombosis in canine coronary arteries. *Circulation* 2001;104:820-5.
- [28] Wang K, Zhou X, Zhou Z, Tarakji K, Carneiro M, Penn MS, et al. Blockade of the platelet P2Y₁₂ receptor by AR-C69931MX sustains coronary artery recanalization and improves the myocardial tissue perfusion in a canine thrombosis model. *Arterioscler Thromb Vasc Biol* 2003;23:357-62.
- [29] Cullen P, Baetta R, Bellosta S, Bernini F, Chinetti G, Cignarella A, et al. Rupture of the atherosclerotic plaque: does a good animal model exist? *Arterioscler Thromb Vasc Biol* 2003;23:535-42.
- [30] Day SM, Reeve JL, Myers DD, Fay WP. Murine thrombosis models. *Thromb Haemost* 2004;92:486-94.
- [31] Opie LH. Glucose and the metabolism of ischaemic myocardium. *Lancet* 1995;345:1520-1.